Editors' Suggestion   Featured in Physics

Determination of the Thermomigration Force on Adatoms

F. Leroy[*], A. El Barraj, F. Cheynis, P. Müller, and S. Curiotto

Aix Marseille Univ, CNRS, CINAM, AMUTECH, Marseille, France

Thermal gradients in nanomaterials can cause surface mass transport phenomena. However, the atomic fluxes are challenging to quantify and the underlying atomic mechanisms are complex. Using low energy electron microscopy we have examined *in operando*, under a thermal gradient of 10^4 K/m, the thermomigration of supercooled Si(111)-1×1 advacancy islands. The islands move in the direction of the thermal gradient at 0.26 ± 0.06 nm/s. This reveals that the adatoms move toward the cold region and the effective force exerted on Si adatoms is $1.4 \pm 0.4 \times 10^{-8}$ eV/nm. We quantify the heat of transport of Si atoms $Q^* = 1.2 \pm 0.4$ eV and show that it corresponds to the combined effects of adatom creation at step edges and adatom diffusion on atomically flat terraces.

The random processes of atomic diffusion in materials are modified under a thermal gradient. This phenomenon is known under different terms, Soret effect, thermophoresis, or thermomigration. This effect was first evidenced historically in homogeneous mixtures of atoms that become heterogeneous in a thermal gradient. In solids it has been shown that vacancies can displace toward higher or lower temperature regions, depending on their formation and diffusion energy barriers, while interstitial atoms displace toward lower temperature regions [1–4]. At least three different phenomena have been proposed to contribute to thermomigration [5]: (i) an intrinsic thermal mass transport phenomenon based on the change of atomic diffusion coefficient between the high and low temperature regions; (ii) a phonon contribution, due to scattering of phonons by mobile atoms; and (iii) the momentum transfer from heat carriers (charges) to mobile atoms.

Thermomigration is often considered as an undesirable phenomenon, because it affects the stability of materials by changing the atomic composition [6]. On the other hand, the fabrication of nanomaterials whose shape, composition, and position is tunable on demand is very appealing. In this context, the application of external fields during the fabrication steps of nanomaterials has been considered. For instance, electric fields have been used to fabricate nanojunctions [7,8] or to modify surface morphologies [9,10]. Thermal gradients have also been demonstrated to activate directed transport of mass along nanotubes [11] or nanowires [12]. Recently, a strategy has been proposed to control the shape of a nanostructure by applying a macroscopic external field such as a thermal gradient [13]. These spectacular phenomena are, however, poorly understood especially for nanostructures. The linear response theory applied to the study of out-of-equilibrium phenomena of mass transport has established the coupling between atomic diffusion and external fields via the phenomenological

Onsager physical coefficients [14]. However, these coefficients, such as the heat of transport that drives species diffusion under a thermal bias, are extremely difficult to measure experimentally and also to evaluate from quantum mechanics basic principles. A successful approach to quantify mass transport phenomena consists in studying atomic step motion as they are abundant structures at surfaces and they play a key role in mass transfers. In particular, the capillary or electromigration forces have been studied by addressing the spatiotemporal fluctuations of the position of isolated or interacting steps [15–17] or by considering the step displacement velocity [18–21]. These results are based on the modeling of the interplay between the atomic migration mechanisms and the velocity of migrating steps. This point is far from being trivial [22–24] since the limiting atomic transport mechanism and the boundary conditions for mass exchanges are usually unknown. The description of this interplay is not only the corner stone for the evaluation of the forces on atoms, it also paves the way for new strategies for nanostructures manipulation [25–27].

In this Letter, we propose to quantify the thermomigration force exerted on adatoms by measuring the surface atomic flux when a thermal gradient is applied. The step motion is used to detect and quantify the atomic fluxes. We have applied this method to quantify the thermomigration force on Si adatoms on the Si(111) surface. We have achieved two essential conditions: (i) atomic motion occurs predominantly at the interior of a confined 2D space closed by a single step edge (a 2D advacancy island) via a large difference of adatom diffusivity between the interior and exterior and (ii) the driving force is induced by a linear thermal gradient to bias the atomic migration. By measuring the drift velocity of 2D islands induced by a thermal gradient, we determine the effective force acting on adatoms. This study is based on *in operando* observations

of island motion on Si(111) surface. The experimental setup uses low energy electron microscopy (LEEM) that allows studying the spatiotemporal dynamics of mass transfers at atomic step level [28]. From the kinetics of mass transfers we deduce that the effective heat of transport of the Si adatoms at the surface is 1.2 ± 0.4 eV. We attribute this heat of transport to the combined effects of the creation of Si adatoms at step edges and Si adatom surface diffusion on the Si(111) atomic plane.

The experiments are performed in an ultrahigh vacuum (UHV) setup equipped with a low energy electron microscope (LEEM III, Elmitec GmbH) [28]. Si(111) substrates (n or p doped, $\rho = 1\ \Omega\,\text{cm}$, $9 \times 9\ \text{mm}^2$ sample size) are rinsed with acetone and ethanol before introduction in UHV. A thermal gradient is applied to the sample close to the $[\bar{1}\,\bar{1}\,2]$ (or $[1\bar{1}0]$) direction using a heating W filament placed behind the sample on one side and a Mo plate placed at the opposite side acting as a heat sink (see Supplemental Material, Sec. 1 [29]). The local temperature is measured with an Impac pyrometer that has been calibrated using the Si(111)-(1×1) to Si(111)-(7×7) surface phase transition occurring in the temperature range 1103–1133 K. The measured thermal gradient is $1.3 \pm 0.2 \times 10^4$ K/m. The Si sample is degassed in UHV for several hours at about 1000 K and then flashed above 1500 K for a few seconds. Extended advacancy islands ($\sim$1 μm) are created by Si sublimation in the middle of large terraces [30]. The surface evolution under thermomigration is studied by LEEM in bright field mode, using a sample bias of 0.5 eV.

LEEM images in Fig. 1(a) show the migration of a Si(111)-(1×1) advacancy island on a Si(111) surface. The Si(111)-(7×7) [Si(111)-(1×1)] surface reconstruction appears with a bright [dark] contrast. Upon slow cooling, by decreasing the heating power, the low temperature Si(111)-(7×7) surface reconstruction nucleates at step edges on the upper terraces [Fig. 1(a)-i] [31] and progressively spreads onto the whole surface [Figs. 1(a)-ii and 1(a)-iii]. Since the crystallographic structures of different (7×7)-reconstructed domains do not necessarily match, the (1×1) phase boundaries are created at their intersections and are pinned at step edges. Contrary to the upper step edge, the nucleation of the (7×7) phase is strongly delayed at the lower step edge and in the middle of the terrace [19]. Therefore the advacancy island stays in a metastable supercooled Si(111)-(1×1) state [see Figs. 1(a)-i–1(a)-iv] [32]. This effect was originally described as a hysteresis of the $(1 \times 1) \leftrightarrow (7 \times 7)$ phase transition temperature [33]. Since the linear thermal gradient is $1.3 \pm 0.2 \times 10^4$ K/m, the temperature difference between two opposite sides of the advacancy island along the thermal gradient is 0.04 K (distance $\sim$3 μm). It is small enough to keep the advacancy island in the (7×7) and (1×1) coexistence range. Figures 1(a)-iii and 1(a)-iv show that the supercooled advacancy island migrates in the direction of the thermal gradient. The
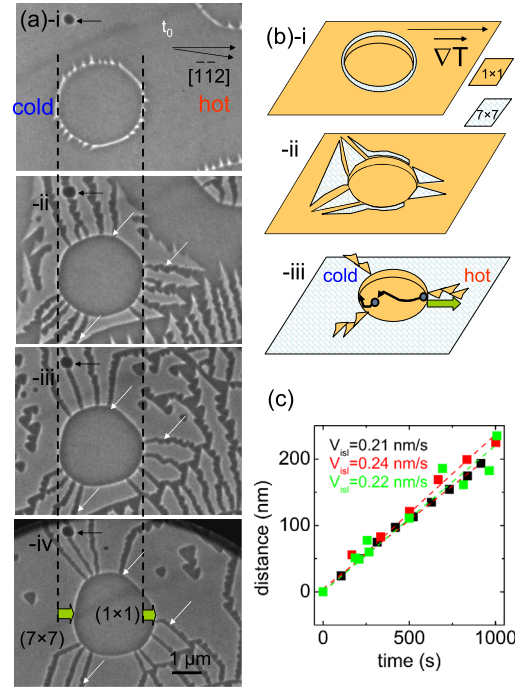

FIG. 1. (a) Sequence of four LEEM images of a Si(111)-(1×1) supercooled advacancy island on a Si(111)-(7×7) surface under a thermal gradient (see complete Movie S2 in Supplemental Material [29]). (a)-i: slow decay of temperature below $(1 \times 1) \leftrightarrow (7 \times 7)$ phase transition temperature to induce the nucleation of the (7×7) surface reconstruction at the upper step edge of the island (1133 K). (a)-ii: expansion of the (7×7) on the whole upper terrace (1103 K). (a)-iii,(a)-iv: occurrence of a steady state thermomigration motion of the advacancy island close to the $[\bar{1}\,\bar{1}\,2]$ direction ($12 \pm 5°$ upward), i.e., along the thermal gradient (hot region). Si(111)-(1×1) out-of-phase boundaries at the (7×7) domain intersections are pinned at the island edge (see white arrows). Black arrows show an immobile defect at the surface that is used to correct the island position from the sample thermal drift. Sample bias for LEEM imaging: $E = 0.5$ eV. The image is slightly under focus to improve the contrast. (b) Scheme of the surface evolution under thermomigration. (c) Time evolution of the displacement of advacancy islands. The steady velocity of the center of mass is 0.21 ± 0.02 nm/s (black squares). Red and green squares correspond to the displacement of two additional islands (see, respectively, Supplemental Material Secs. 3 and 4 [29]).

initial phase boundaries, attached at the step edge of the island, follow the island displacement. After a transitory stage, due to sample thermalization and expanding of the (7×7) surface reconstruction, the island migrates in a steady state with a slight facetting of the so-called unfaulted step edges perpendicular to the $\langle 11\bar{2} \rangle$ direction [34]. During $\sim$900 s, the advacancy island moves $\sim$190 nm and the average velocity of the center of mass is constant: $V_{\text{isl}} = 0.21 \pm 0.02$ nm/s. The study of the thermomigration of many islands shows no size dependence and an average velocity and deviation $V_{\text{isl}} = 0.26 \pm 0.06$ nm/s (see Movie S3 in Supplemental Material [29]). Similar results are also

obtained considering, for instance, the $[1\bar{1}0]$ direction for the thermal gradient (see Movie S4 in Supplemental Material [29]). From the lack of size dependency of the velocity, we can deduce that terrace diffusion is the dominant atomic transport mechanism of Si adatoms [24]. This result corroborates previous measurements obtained at and above the $(1 \times 1) \leftrightarrow (7 \times 7)$ phase transition temperature [20]. Let us note that the mechanism of periphery diffusion of adatoms along the step edge is negligible since the velocity should decay as $1/R$ (R is the island radius) [21,35], and no evidence of such a behavior is observed. In addition, attachment and detachment (AD) processes at step edges are comparatively very fast since for AD limited kinetics the velocity should increase linearly with the island size [35]. This is also in accordance with a kinetic length of attachment-detachment of a few hundreds of nanometers whereas the island size is > 1 µm [20]. Then the terrace diffusion mechanism of Si adatoms may occur outside the island, i.e., on the upper (7×7) terrace, and/or inside the island, i.e., on the lower (1×1) terrace. As shown by Hibino *et al.* [19,36], the surface diffusivity of Si adatoms on the (1×1) is much larger than on the (7×7) (ratio ~ 20). Therefore we can conclude that in the super-cooled state, the limiting mass transport phenomenon of the advacancy island is terrace diffusion inside the island, i.e., in a confined area limited by a single atomic step. The resulting island drift velocity V_{isl} reads

$$V_{\text{isl}} = \frac{c_{\text{eq}}}{1 - c_{\text{eq}}} v_{\text{ad}}, \qquad (1)$$

where c_{eq} is the equilibrium surface concentration of mobile adatoms and v_{ad} is the adatom's velocity on the (1×1) terrace. The $[1/(1 - c_{\text{eq}})]$ term corrects the velocity with advection [37], i.e., the sweeping effect on the adatoms due to the step motion. To estimate the adatom velocity v_{ad} we have to determine c_{eq}. We have previously shown that there is 0.24 ± 0.04 monolayer of adatoms on the (1×1) surface of the advacancy island [21]. This result is similar to the adatom concentration on a (1×1) surface even though here the step edge is hybrid, i.e., (1×1) reconstructed on the lower terrace and (7×7) on the upper one. This observation is thermodynamically consistent since the equilibrium concentration of adatoms on a terrace is related to a difference of energy between two states: an atom attached at a step edge and on a terrace (adatom). As the chemical environments of an atom at a (7×7) or a (1×1) step edge are similar and very distinct from an adatom on top of a (1×1) terrace, we expect that the step edge reconstruction only slightly modifies the equilibrium concentration. We derive finally the adatom velocity $v_{\text{ad}} = 1.9 \pm 0.4$ nm/s on the (1×1) surface reconstruction at 1103 K. Let us note that the step edge on Si(111) is a bilayer; therefore the considered equilibrium concentration c_{eq} in Eq. (1) is 0.12 ± 0.02 bilayer. In

the framework of the linear response theory, considering a weak thermomigration force [24], this velocity derives from the Einstein relation $v_{\text{ad}} = (\Omega D/k_B T)F$, where k_B is the Boltzmann constant, T the temperature, $\Omega = 0.064$ nm^2 the atomic area, D the diffusion coefficient, and F the thermomigration force. Therefore the force F on Si adatoms can be obtained since the diffusion coefficient D is known. Hibino *et al.* have found $Dc_{\text{eq}} = 3.0 \times 10^7$ s^{-1} [19,32] at the phase transition temperature. Pang *et al.* have obtained by different approaches $Dc_{\text{eq}} = 1.8 \pm 0.4 \times 10^7$ s^{-1} [20] in a slightly higher temperature regime (1163 K). Considering an average value for D we can deduce the amplitude of the thermomigration force $F = 1.4 \pm 0.4 \times 10^{-8}$ eV/nm. The aforementioned hypothesis of a weak thermomigration force is validated *a posteriori* by comparing the thermomigration length $\xi = k_B T/F = 6.8$ mm with the interatomic distance $a = 0.384$ nm.

We propose in the following a modeling of the thermomigration process of the island in the framework of a one-dimensional Burton-Cabrera-Frank model [38]. We assume a thermally activated process of diffusion on a terrace limited by two step edges [see Fig. 2(a)]. Since the temperature is not homogeneous at the sample surface, the adatoms experience a change of jump frequency along the thermal gradient [2]. Considering a jump frequency $\nu = \nu_0 e^{-E_d/k_B T}$, where ν_0 is a prefactor and E_d is the diffusion energy barrier, the adatom velocity along the thermal gradient is [Fig. 2(b)]

$$v_{\text{ad}} = a[\nu(T) - \nu(T + \delta T)] = \frac{a^2 \nu_0 e^{-E_d/k_B T}}{k_B T} \left[\frac{-E_d}{T} \frac{\delta T}{a}\right], \qquad (2)$$

where δT is the difference of temperature between two neighboring atomic sites at distance a and $(\delta T/a)$ is the thermal gradient. We can identify Eq. (2) with the Einstein relation, and $\vec{F} = -(E_d/T)\overrightarrow{\nabla T}$ is the thermomigration force. This force originates from the change of diffusion coefficient along the thermal gradient and is directed toward the cold side. Considering that more generally the thermomigration force reads $\vec{F} = -(Q^*/T)\overrightarrow{\nabla T}$, where
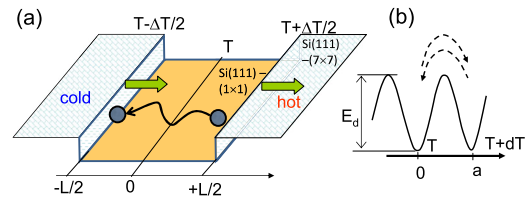

FIG. 2. (a) Scheme of the mass transfer process: detachment of atoms from the step at the hot side, biased terrace diffusion and attachment of atoms at the step (cold side). (b) Model of atomic jump in the direction opposite to the thermal gradient .

Q^* is the heat of transport that drives the atomic transport, Q^* is the diffusion energy barrier of adatoms E_d. Since the adatoms are migrating opposite to the thermal gradient, the advancy island migrates toward the hot side, as observed experimentally for the Si(111)-(1 × 1) advancy islands. In this 1D model the step edges control the boundary conditions: at the hot side, the step is acting as an adatom source, and at the cold side, the step is an adatom sink. Since the attachment and detachment processes of adatoms at step edges are not limiting the island motion, we assume that the kinetics of atomic transfers is infinitely fast and the local concentration of adatoms at step edges is thus at equilibrium. Nevertheless, the two opposite step edges have a temperature offset ΔT due to the thermal gradient [see Fig. 2(a)]. Then the equilibrium adatom concentration is higher on the hot side than on the cold side. Considering that the equilibrium concentration is also given by a thermally activated process $c_{eq} = c_0 e^{-E_c/k_B T}$, where c_0 is a prefactor and E_c is the creation energy barrier of adatoms at step edges, we obtain the island velocity in the steady state regime (see Sec. 5 in Supplemental Material [29]):

$$\vec{V}_{isl} = \frac{D c_{eq} \Omega}{(1 - c_{eq}) k_B T} \left[-\frac{E_d + E_c}{T} \overrightarrow{\nabla T} \right]. \qquad (3)$$

The resulting effective force on the adatoms is $\vec{F} = -[(E_d + E_c)/T] \overrightarrow{\nabla T}$, and the deduced heat of transport, $Q^* = E_d + E_c$, has two contributions: the diffusion energy barrier on the terrace and the creation energy of adatoms at step edges. Since we have experimentally evaluated the thermomigration force F, we can now deduce the heat of transport $Q^* = -F(T/\nabla T) = 1.2 \pm 0.4$ eV and compare with $E_d + E_c$ as derived from our Burton-Cabrera-Frank-based model [38] of island velocity under thermomigration. The sum $E_d + E_c$ has been previously evaluated by Pang et al. (1.53 eV [20]) and Hibino et al. (1.3 eV [19]) in the context of island decay via capillary forces. Other estimation of $E_d + E_c$ based on step edge fluctuation analysis (1.2 eV [39]) or step motion under sublimation conditions (1.9 eV [40]) also show close agreement with Q^*. The measured heat of transport is thus compatible with a dominant flux of adatoms induced by the gradients of diffusion coefficient at the surface and equilibrium concentration of adatoms at step edges. The influence of the heat current carried by the charge carriers and phonon current on adatom's displacement appear to be negligible. This result confirms that our experimental approach is well suited to determine the heat of transport of Si adatoms. Interestingly, such a method has been recently applied in the context of supercooled Si advancy islands on Si(111) but applying an electric field to induce the electromigration phenomenon [21]. Then considering both studies, the ratio of the velocity of thermomigrating islands (V_{isl}^{TM}) and electromigrating islands (V_{isl}^{EM}) is equal to the ratio of the thermal and electric forces applied on adatoms. This ratio allows us to get rid of the measurement of the adatoms' diffusivity and to directly estimate the ratio of two fundamental quantities for Si adatoms, i.e., the heat of transport and the effective valence Z^* (considering that the electric force reads $F^{EM} = eZ^*E$ [41], where e is the electron charge and E the applied electric field), then

$$\frac{Q^*}{Z^*} = \frac{-F^{TM} \frac{T}{\nabla T}}{\frac{F^{EM}}{eE}} = -\left[\frac{V_{isl}^{TM}}{V_{isl}^{EM}} \right] \left[\frac{eET}{\nabla T} \right], \qquad (4)$$

and we deduce from Ref. [21] that $(Q^*/Z^*) = -0.7 \pm 0.2$ eV for Si adatoms.

Let us note that our approach of step motion measurement to estimate the force exerted on adatoms is based on the presence of an asymmetry between both sides of an atomic step. This asymmetry is expected in most systems due to the Ehrlich-Schwoebel barrier [42,43]: the energy barriers for uphill and downhill diffusion at a step edge have no reason to be same even though the energy difference may be small. Moreover, systems with different surface termination on both sides of a step edge are good candidates to evaluate the thermomigration force since the adatom diffusivity is strongly modified by the surface structure.

In conclusion, we have observed and described at the atomic level the thermomigration phenomenon on the Si (111) surface. The study of the atomic transport mechanisms is based on the characterization of the migration of adatoms confined in a 2D space. Using a supercooled state of the Si(111) surface, we have been able to maintain an advancy island in the (1 × 1) high temperature state surrounded by the (7 × 7) low temperature state. Thanks to the large difference of atomic diffusivity of both surface structures, this regime allows keeping the atomic exchanges only inside the 2D island. By measuring the island velocity with in operando LEEM, under a thermal gradient, and analyzing the migration processes, we show the following. (i) Si adatom migration on the Si(111)-(1 × 1) terrace is biased in the direction opposite to the thermal gradient. (ii) Extremely small forces exerted on adatoms can be quantified: $F = 1.4 \pm 0.4 \times 10^{-8}$ eV/nm. (iii) The fundamental heat of transport is deduced: $Q^* = 1.2 \pm 0.4$ eV and attributed to the diffusion energy and creation energy barriers of adatoms. We hope that this experimental work will be a benchmark for further experimental and theoretical investigations on the surface dynamics of mass transfers in the presence of a thermal gradient.

*frederic.leroy.3@univ-amu.fr

[1] W. Shockley, Some predicted effects of temperature gradients on diffusion in crystals, Phys. Rev. **91,** 1563 (1953).

[2] J. A. Brinkman, The effect of temperature gradients on diffusion in crystals, Phys. Rev. **93,** 345 (1954).

[3] A. D. LeClaire, Some predicted effects of temperature gradients on diffusion in crystals, Phys. Rev. **93,** 344 (1954).

[4] T. Y. Tan, Mass transport equations unifying descriptions of isothermal diffusion, thermomigration, segregation, and position-dependent diffusivity, Appl. Phys. Lett. **73,** 2678 (1998).

[5] H. B. Huntington, Driving forces for thermal mass transport, J. Phys. Chem. Solids **29,** 1641 (1968).

[6] A. T. Huang, A. M. Gusak, K. N. Tu, and Y. S. Lai, Thermomigration in SNPB composite flip chip solder joints, Appl. Phys. Lett. **88,** 141911 (2006).

[7] R. Hoffmann-Vogel, Electromigration and the structure of metallic nanocontacts, Appl. Phys. Rev. **4,** 031302 (2017).

[8] Valentin Dubois, Shyamprasad N. Raja, Pascal Gehring, Sabina Caneva, Herre S. J. van der Zant, Frank Niklaus, and Goran Stemme, Massively parallel fabrication of crack-defined gold break junctions featuring sub-3 nm gaps for molecular devices, Nat. Commun. **9,** 3433 (2018).

[9] F. Leroy, P. Müller, J. J. Metois, and O. Pierre-Louis, Vicinal silicon surfaces: From step density wave to faceting, Phys. Rev. B **76,** 045402 (2007).

[10] F. Leroy, D. Karashanova, M. Dufay, J. M. Debierre, T. Frisch, J. J. Métois, and P. Müller, Step bunching to step-meandering transition induced by electromigration on Si (111) vicinal surface, Surface Sci. **603,** 507 (2009).

[11] Amelia Barreiro, Riccardo Rurali, Eduardo R. Hernandez, Joel Moser, Thomas Pichler, Laszlo Forro, and Adrian Bachtold, Subnanometer motion of cargoes driven by thermal gradients along carbon nanotubes, Science **320,** 775 (2008).

[12] Qian Liu, Rujia Zou, Jianghong Wu, Kaibing Xu, Aijiang Lu, Yoshio Bando, Dmitri Golberg, and Junqing Hu, Molten Au/Ge alloy migration in Ge nanowires, Nano Lett. **15,** 2809 (2015).

[13] Francesco Boccardo and Olivier Pierre-Louis, Controlling the Shape of Small Clusters with and without Macroscopic Fields, Phys. Rev. Lett. **128,** 256102 (2022).

[14] Lars Onsager, Reciprocal relations in irreversible processes. I., Phys. Rev. **37,** 405 (1931).

[15] N. C. Bartelt, J. L. Goldberg, T. L. Einstein, Ellen D. Williams, J. C. Heyraud, and J. J. Métois, Brownian motion of steps on Si(111), Phys. Rev. B **48,** 15453 (1993).

[16] D. B. Dougherty, I. Lyubinetsky, E. D. Williams, M. Constantin, C. Dasgupta, and S. Das Sarma, Experimental Persistence Probability for Fluctuating Steps, Phys. Rev. Lett. **89,** 136102 (2002).

[17] O. Bondarchuk, W. G. Cullen, M. Degawa, E. D. Williams, T. Bole, and P. J. Rous, Biased Surface Fluctuations due to Current Stress, Phys. Rev. Lett. **99,** 206801 (2007).

[18] K. Thurmer, J. E. Reutt-Robey, E. D. Williams, M. Uwaha, A. Emundts, and H. P. Bonzel, Step Dynamics in 3D Crystal Shape Relaxation, Phys. Rev. Lett. **87,** 186102 (2001).

[19] H. Hibino, C.-W. Hu, T. Ogino, and I. S. T. Tsong, Decay kinetics of two-dimensional islands and holes on Si(111) studied by low-energy electron microscopy, Phys. Rev. B **63,** 245402 (2001).

[20] A. B. Pang, K. L. Man, M. S. Altman, T. J. Stasevich, F. Szalma, and T. L. Einstein, Step line tension and step morphological evolution on the Si(111) (1×1) surface, Phys. Rev. B **77,** 115424 (2008).

[21] F. Leroy, A. El Barraj, F. Cheynis, P. Müller, and S. Curiotto, Electric forces on a confined advacancy island, Phys. Rev. B **102,** 235412 (2020).

[22] S. Curiotto, P. Müller, A. El-Barraj, F. Cheynis, O. Pierre-Louis, and F. Leroy, 2D nanostructure motion on anisotropic surfaces controlled by electromigration, Appl. Surf. Sci. **469,** 463 (2019).

[23] P. Kuhn, J. Krug, F. Hausser, and A. Voigt, Complex Shape Evolution of Electromigration-Driven Single-Layer Islands, Phys. Rev. Lett. **94,** 166105 (2005).

[24] O. Pierre-Louis and T. L. Einstein, Electromigration of single-layer clusters, Phys. Rev. B **62,** 13697 (2000).

[25] A. Kumar, D. Dasgupta, and D. Maroudas, Complex Pattern Formation from Current-Driven Dynamics of Single-Layer Homoepitaxial Islands on Crystalline Conducting Substrates, Phys. Rev. Appl. **8,** 014035 (2017).

[26] S. Curiotto, F. Cheynis, P. Müller, and F. Leroy, 2D manipulation of nanoobjects by perpendicular electric fields: Implications for nanofabrication, ACS Appl. Nano Mater. **3,** 1118 (2020).

[27] Yun-Ran Wang, Im Sik Han, Chao-Yuan Jin, and Mark Hopkinson, Formation of laterally ordered quantum dot molecules by *in situ* nanosecond laser interference, Appl. Phys. Lett. **116,** 201901 (2020).

[28] F. Cheynis, F. Leroy, A. Ranguis, B. Detailleur, P. Bindzi, C. Veit, W. Bon, and P. Müller, Combining low-energy electron microscopy and scanning probe microscopy techniques for surface science: Development of a novel sample-holder, Rev. Sci. Instrum. **85,** 043705 (2014).

[29] See Supplemental Material at http://link.aps.org/supplemental/10.1103/PhysRevLett.131.116202 for a detailed description of the sample holder dedicated to thermomigration and thermal gradient measurements (Sec. 1); a LEEM movie of the thermomigration of a Si(111)-(1×1) advacancy island on Si(111) surface in a direction close to $[\bar{1}\,\bar{1}\,2]$ with sample bias 0.5 eV, total duration 1572 s, and field of view 7.6×6 μm^2 (Sec. 2); Sec. 3: Same as Sec. 2 with total duration 2685 s and field of view 6.6×5.8 μm^2; Sec. 4: Same as Sec. S2 with a thermal gradient along $[\bar{1}10]$ with steady state island velocity 0.22 ± 0.05 nm/s, total duration 4147 s, and field of view 4.2×4.2 μm^2; and modeling of the island velocity in the framework of the Burton-Cabrera-Frank model and including a thermal gradient (Sec. 5).

[30] Y. Homma, H. Hibino, T. Ogino, and N. Aizawa, Sublimation of the Si(111) surface in ultrahigh vacuum, Phys. Rev. B **55,** R10237 (1997).

[31] N. Osakabe, Y. Tanishiro, K. Yagi, and G. Honjo, Direct observation of the phase-transition between the (7×7) and (1×1) structures of clean (111) silicon surfaces, Surf. Sci. **109,** 353 (1981).

[32] H. Hibino, Y. Watanabe, C.-W. Hu, and I. S. T. Tsong, Thermal decay of superheated 7×7 islands and supercooled "1×1" vacancy islands on Si(111), Phys. Rev. B **72,** 245424 (2005).

[33] C.-W. Hu, H. Hibino, T. Ogino, and I. S. T. Tsong, Hysteresis in the (1×1)-(7×7) first-order phase transition on the Si(111) surface, Surf. Sci. **487,** 191 (2001).

[34] H. Tochihara, W. Shimada, M. Itoh, H. Tanaka, M. Udagawa, and I. Sumita, Structure and restructuring of the atomic steps on Si(111) 7×7, Phys. Rev. B **45**, 11332 (1992).

[35] H. C. Jeong and E. D. Williams, Steps on surfaces: Experiment and theory, Surf. Sci. Rep. **34**, 171 (1999).

[36] H. Hibino, C.-W. Hu, T. Ogino, and I. S. T. Tsong, Diffusion barrier caused by 1×1 and 7×7 on Si(111) during phase transition, Phys. Rev. B **64**, 245401 (2001).

[37] F. Hausser, P. Kuhn, J. Krug, and A. Voigt, Morphological stability of electromigration-driven vacancy islands, Phys. Rev. E **75**, 046210 (2007).

[38] W. K. Burton, N. Cabrera, F. C. Frank, and Nevill Francis Mott, The growth of crystals and the equilibrium structure of their surfaces, Phil. Trans. R. Soc. A **243**, 299 (1951).

[39] A. Pimpinelli, J. Villain, D. E. Wolf, J.-J. Métois, J.-C. Heyraud, I. Elkinani, and G. Uimin, Equilibrium step dynamics on vicinal surfaces, Surf. Sci. **295**, 143 (1993).

[40] Yoshikazu Homma, Hiroki Hibino, Toshio Ogino, and Noriyuki Aizawa, Sublimation of a heavily boron-doped Si(111) surface, Phys. Rev. B **58**, 13146 (1998).

[41] H. B. Huntington and A. R. Grone, Current-induced marker motion in gold wires, J. Phys. Chem. Solids **20**, 76 (1961).

[42] Richard L. Schwoebel and Edward J. Shipsey, Step motion on crystal surfaces, J. Appl. Phys. **37**, 3682 (1966).

[43] Gert Ehrlich and F. G. Hudda, Atomic view of surface self-diffusion: Tungsten on tungsten, J. Chem. Phys. **44**, 1039 (1966).